

Does Continual Learning = Catastrophic Forgetting?

Anh Thai, Stefan Stojanov, Isaac Rehg, James M. Rehg
Georgia Institute of Technology

{athai6, sstojanov, isaacrehg, rehg}@gatech.edu

Abstract

Continual learning is known for suffering from catastrophic forgetting, a phenomenon where earlier learned concepts are forgotten at the expense of more recent samples. In this work, we challenge the assumption that continual learning is inevitably associated with catastrophic forgetting by presenting a set of tasks that surprisingly do not suffer from catastrophic forgetting when learned continually. The robustness of these tasks leads to the potential of having a proxy representation learning task for continual classification. We further introduce a novel yet simple algorithm, YASS that achieves state-of-the-art performance in the class-incremental categorization learning task and provide an insight into the benefit of learning the representation continuously. Finally, we present converging evidence on the forgetting dynamics of representation learning in continual models. The codebase, dataset and pre-trained models released with this article can be found at <https://github.com/rehg-lab/CLRec>.

1. Introduction

In continual learning (CL), a stream of incrementally-arriving inputs is processed without access to past data. A key challenge is to avoid catastrophic forgetting [47], which arises if previously-learned representations are degraded by more recent exposures. Substantial effort has been made to combat forgetting [16, 68, 34, 24], and it has come to exemplify continual learning. However, past works have explored a surprisingly limited set of tasks, with an almost exclusive focus on classification. In particular, no prior works have addressed *reconstruction* tasks, such as 3D shape estimation from single images.

We demonstrate the surprising finding that a broad set of *continual reconstruction tasks*, including single image 3D shape reconstruction, depth and normal estimation, and image autoencoding, *do not* exhibit catastrophic forgetting (Sec. 3). We believe we are the first to study CL for reconstruction-style tasks such as these. We examine the performance of continual reconstruction in the *repeated*

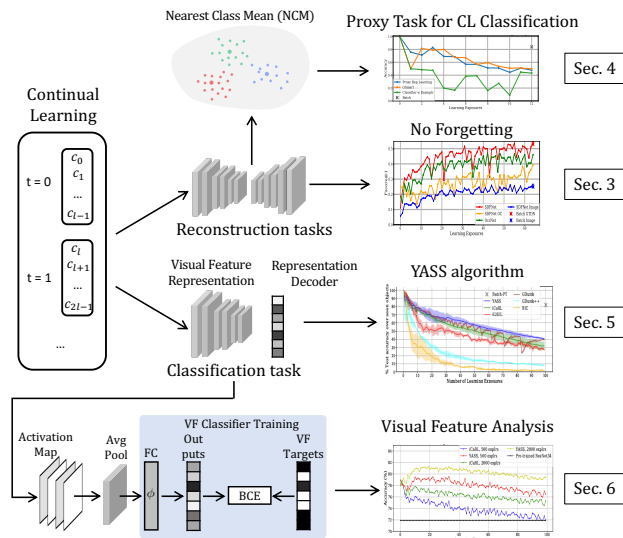


Figure 1: An overview of our four main findings: (Top) CL tasks involving reconstruction do not suffer from forgetting (Sec. 3), and can be used as proxy tasks in a novel CL classification approach that is also robust to forgetting (Sec. 4). (Bottom) YASS is a simple and novel CL classification method that achieves SOTA performance (Sec. 5), and we provide a novel visual feature analysis for studying feature forgetting (Sec. 6).

learning exposures paradigm introduced in [54].¹ We show that when the continual learner is exposed to an object class multiple times in a random order (ie. with repetitions), its performance asymptotically approaches the accuracy of batch learning. In addition, we demonstrate in Sec. 4 that continual reconstruction can serve as an *unsupervised proxy task* for image classification, resulting in a novel continual classification algorithm. Our findings suggest that the challenge of catastrophic forgetting is primarily an issue for classification tasks, and does not extend to all continual learning problems.

A key criterion for successful continual learning (CL) is *positive forward transfer* [35], which arises when representations trained on prior tasks contain useful information for the current task. Forward transfer in continual classification

¹We use the term *learning exposure* to refer to each new increment of data, i.e. the learner’s next “exposure” to the concepts being learned.

is naturally studied in the *class-incremental single-head* setting, where data from a single classification dataset is distributed across a sequence of exposures [36].² While this setting maximizes the opportunities for forward transfer, as classes from the same dataset can often share feature representations, prior work on *continuous representation learning* has identified significant challenges to effective forward transfer, particularly in the single-exposure case where the learner does not get multiple exposures to each class. A common approach [46, 10, 59] uses a continuously-updated feature representation, combined with exemplar memory, to transfer information between tasks.

Recently, the GDumb baseline introduced in [42] has called the effectiveness of forward transfer in CL for classification into question. GDumb is an episodic representation learner, which maintains a set of evolving exemplars but *reinitializes* the feature representation and trains it from scratch during each learning exposure. This approach was shown to outperform prior methods, suggesting that a continuous feature representation approach may not be an effective strategy for achieving forward transfer. We conducted an additional investigation into this phenomenon as it seemed to contradict our findings for continual reconstruction. This resulted in a new baseline continual classification method called YASS (Yet Another Simple baSeline, Sec. 5), which is the *first simple continuous representation approach to achieve comparable performance to GDumb* on multiple class-incremental learning tasks. YASS utilizes a simple method for managing exemplars and ameliorating class imbalance which is surprisingly effective.

In order to shed further light on the mechanisms that lead to catastrophic forgetting in continual classification, we conducted an investigation of the dynamics of continual feature learning (Sec. 6). We provide evidence to support the hypothesis that the FC layer, which decodes the visual feature representation into the class outputs, is more likely to be vulnerable to forgetting than the continually-evolving visual feature representation maintained in a classifier’s convolutional layers (see also [59]). Our analysis is verified by three different tools: CKA [27], FC layer fine-tuning, and a novel task of predicting visual feature outputs corresponding to the final convolutional layer (visual feature analysis)

In summary, this paper makes four contributions:

- *Continual reconstruction* tasks do not suffer from catastrophic forgetting, and repeated exposures [54] lead asymptotically to batch performance (Sec. 3).
- Using reconstruction as a *proxy task* for classification results in a competitive CL method (Sec. 4).
- A novel method for continual classification with simple design choices, called YASS, achieves SOTA performance in different settings (Sec. 5).

²This is the CL task formulation B2 in the taxonomy proposed in [42].

Task	2.5D/3D info required	Dataset
Single-view 3D Shape Rec. 3.1	Yes	ShapeNetCore.v2
Single-view 2.5D Pred. 3.2	Yes	ShapeNetCore.v2
Proxy Task 4	Yes	ShapeNetCore.v2 & ModelNet40
Image Autoenc. 3.3	No	CIFAR-100
Classification 5, 6	No	CIFAR-100 & iNaturalist-2019

Table 1: Summary of the tasks we evaluate and the corresponding datasets used in this paper. ShapeNetCore.v2 [12] and ModelNet40 [60] are used for tasks that require 2.5D or 3D shape information while CIFAR-100 [28] and iNaturalist-2019 [21] are used for tasks that only require RGB images.

- Analysis of the evolving feature representation during learning demonstrates that forgetting disproportionately affects the FC layer during continual classifier learning, verified by three different tools (Sec. 6).

Taken collectively, these findings suggest that *continual learning is not synonymous with catastrophic forgetting*, and the extent to which forgetting occurs depends upon the nature of the the task (classification vs. reconstruction), the data distribution (e.g. the single- vs multiple-exposure case), and the strategy for forward transfer (continual vs episodic representation learning).

2. Related Work

Our work is most closely-related to four bodies of prior work: 1) CL works outside of the image classification paradigm (relevant to our findings on CL for reconstruction), 2) CL works on image classification (relevant to our YASS method and our approach to using reconstruction as a CL proxy task), 3) Methods for analyzing feature representations (relevant to our visual feature analysis), and 4) Models for single image 3D shape reconstruction that form the basis of our CL approach.

CL of Non-Classification Tasks: We are the first to investigate 3D shape reconstruction from images in a CL setting. This is also the first demonstration of a set of CL tasks that is intrinsically robust to catastrophic forgetting. While most prior CL works have addressed image classification, a few prior works have addressed various other tasks: Aljundi et al. [4] studied the problem of actor face tracking in video, while [38, 11] explored image segmentation. Shmelkov et al. [52] and Liu et al. [33] investigated incremental object detection while [30, 57] learned image generation. Elhoseiny et al. [19] examined continual fact learning by utilizing a visual-semantic embedding. Others [1, 25, 62] focused on reinforcement learning task. *All of these works reported challenges with catastrophic forgetting commensurate with the classification setting.*

CL for Classification: Our work on continual classification is most closely-related to the baseline method GDumb, which was introduced in [42] along with a taxonomy of CL problems and methods. The taxonomy specifies five

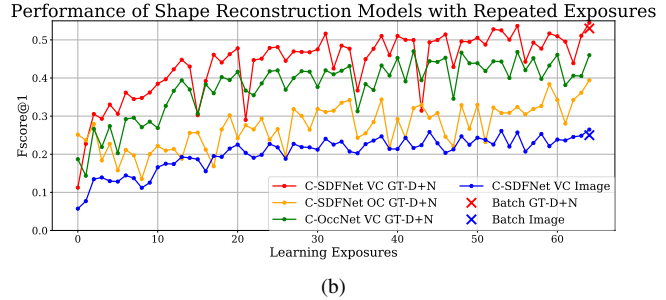
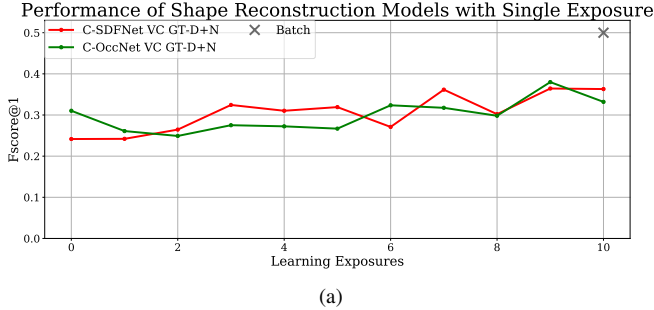


Figure 2: (a) Performance of shape reconstruction methods when presented with a single exposure for each category from all 55 categories of ShapeNetCore.v2, 5 classes/exposure (b) repeated exposures case on ShapeNet13 with 10 repeated exposures, 2 classes/exposure. Catastrophic forgetting does not happen to any of the algorithms in either case.

different formulations based on the assumptions made in CL tasks, such as task-incremental with multi-head output, class-incremental with single-head output, etc. We address formulation B, in which classes are learned incrementally in an offline manner with hard task boundaries, which includes a large number of related works [46, 10, 59, 22, 7, 70, 18, 34, 9]. More specifically, we fall into sub-category B2 where the total classes are divided into different tasks, and trained sequentially with a single head.

Our two contributions relative to prior work in B2 are: 1) YASS baseline method (Sec. 5), and 2) investigation of 3D reconstruction as a proxy task for CL classification (Sec. 4). Compared to prior exemplar-based continuous representation learning methods, such as iCaRL [46], E2EIL [10], and BiC³ [59], the YASS approach is a dramatic simplification, based on random exemplar selection and weighted gradient balancing. We meet or exceed the performance of these methods on CIFAR-100 [28] and iNaturalist [21]. Compared to GDumb [42], the superior performance of YASS on CIFAR-100 (single exposure) and CIFAR-60 (repeated exposures, see Appendix), and comparable performance on iNaturalist, *demonstrates for the first time that a simple continuous representation learning approach outperforms episodic representation learning* when data balancing is maintained and exemplars are managed appropriately.

Our work on a reconstruction-based proxy task for CL classification is unique, but it is peripherally-related to other CL works which explore alternative classification losses or forms of supervision. We share with Yu et al. [66] the use of the nearest-class-mean (NCM) classification rule. We use NCM for classification based on a latent shape representation trained without class supervision, while Yu et al. use NCM for classification in an embedding layer which is trained with ground-truth class labels. Another related work by Rao et al. [45] performs unsupervised CL in a multi-task setting where the boundaries between tasks are unknown. In contrast, our unsupervised training paradigm utilizes 3D

shape reconstruction as a proxy task.

Finally, We note that other works address the multi-task CL setting (form C and D described in [42]): [39, 6, 48, 65, 51, 49, 64, 41, 3, 26, 67, 17], a setting in which GDumb gives competitive performance. These works lie outside the scope of the current paper.

Feature Representation Analysis: Our work on the visual feature analysis is also related to an additional body of work that visualizes and analyzes the representations produced by CL. Approaches use CKA [44] and CCA [32] to compare the representations produced by different convolutional layers after being trained on new classes. Other works have investigated the dynamics of *batch* learning [31, 43, 27, 40]. Some others attempt to train classifiers at each layer in a deep model and observe the linear separability of the learned features [2] or specifically focus on the invariance and equivariance of individual representations [29]. A related work by Chaudhry et al. [13] introduces LCA as a metric to quantify the convergence rate of learning algorithms. Wu et al. [59] share our observation of the impact of catastrophic forgetting on the FC layer relative to the feature representation (conv layers).

We complement these prior methods by providing a means to explicitly quantify the robustness of the representation learned independently from the classifier over time. In particular, we compare the similarity of the feature representation extracted from the pooling layer before the final FC layer to that produced by the model trained to convergence on all training data (batch model).

Batch-Mode 3D Shape Reconstruction: Our CL reconstruction work in Sec. 3 is based on two prior works on single image 3D shape reconstruction: SDFNet [56] and OccNet [37]. Past work has shown that models trained with a viewer-centered (VC) coordinate system learn a more general shape representation than the object-centered (OC) approach [69, 50, 56]. We investigate the CL behavior of 3-DOF VC and OC approaches and provide further evidence for the superiority of 3-DOF VC.

³We use the PyTorch implementation of this method at <https://github.com/sairin1202/BIC>

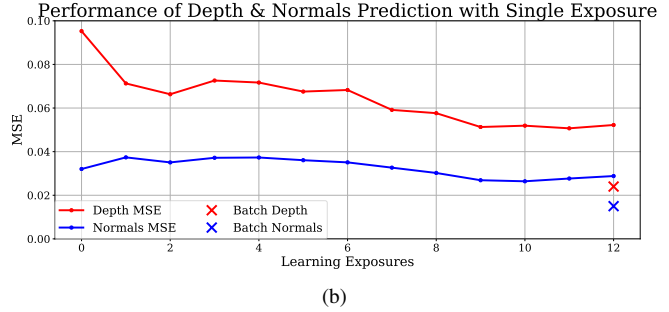
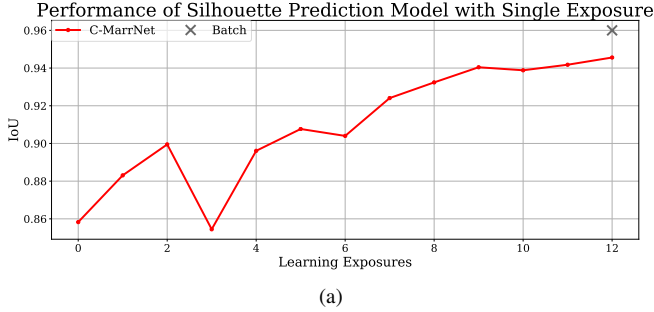


Figure 3: (a) Performance in terms of IoU of silhouette prediction model, the higher the IoU the better, (b) MSE loss of depth and normals prediction model on ShapeNet13 in single exposure setting, 1 class/exposure, the lower the MSE loss the better. The performance of CL models approaches batch in both cases.

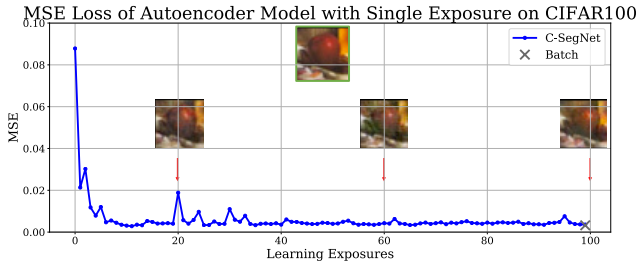


Figure 4: MSE loss when training the autoencoder continually on CIFAR-100, single exposure. The lower the MSE loss the better. The top image with green boundary is a ground truth test sample from the first category. The images on the bottom are the predicted results of the continual model at exposure 20, 60, 100 respectively. The CL model is able to reconstruct the sample image from the first class well even without seeing the learned categories again in later learning exposures.

3. Reconstruction Tasks Do Not Suffer from Catastrophic Forgetting

In this section, we present a set of tasks that take a single image as input and output a reconstruction of the scene. We demonstrate that, unlike classification tasks, reconstruction does not suffer from catastrophic forgetting (Fig. 1, second row). It is important to emphasize that the “continual learning” algorithm used in this section is standard SGD run on each learning exposure with continuous representation learning. In other words, *we do not need to utilize additional losses, external memory, or other methods to achieve good continual learning performance*. This is in stark contrast to the situation for the classification CL task.

We present results for both single and repeated exposures. In the *single exposure* setting, which is the standard approach to class-incremental learning, object classes are presented sequentially and the learner sees each object category exactly once. In the *repeated exposure* setting, each class occurs a fixed number of times (e.g. 10 repetitions) in random order.⁴ This is a more realistic setting for many

⁴In the case of 50 classes repeated 10 times, we would first generate 500 learning exposures, and then perform a random permutation to obtain the order seen by the learner. As a result, classes repeat in complex and highly-variable patterns. Note that even though classes repeat, each learn-

ing exposure still contains only a single class (or a small number), thereby preserving the domain shift between exposures that makes CL challenging.

3.1. Single-view 3D Shape Reconstruction

Approach. We adapt SDFNet [56] and OccNet [37] for CL in both single and repeated exposure settings, termed C-SDFNet and C-OccNet respectively. We train both methods with the 3-DOF VC representation (varying in azimuth, elevation and camera tilt) from [56], which was shown to give the best generalization performance.⁵ We train both models with ground truth depth and normals (2.5D sketches) as input, a setting we denote as GT D+N. This allows the model to achieve higher accuracy, making it easier to observe any issues due to forgetting. We additionally train C-SDFNet in the repeated exposures case with OC representation, in which the model is trained to output the shape in the canonical pose, and with RGB image inputs (denoted as Image).

Datasets & Metric. We learn on all 55 classes of ShapeNetCore.v2 (52K instances) with 5 classes per exposure for the single exposure case, and on the largest 13 classes of ShapeNetCore.v2 (40K meshes), which we denote as ShapeNet13, with 2 classes per exposure for the repeated exposure case. Note that ShapeNetCore.v2 is currently the largest shape dataset with category labels and ShapeNet13 is commonly used in 3D shape reconstruction works because of the outnumbered instances compared to the remaining classes. Each exposure is generated by utilizing all of the samples from the training split of each category currently present⁶. Following prior works in shape reconstruction [56, 63, 55], we utilize F-Score at 1% (FS@1) as our main evaluation metric. We report the average FS@1

⁵SDFNet with 3-DOF VC is the current SOTA for single image 3D shape reconstruction.

⁶For instance, if chair and table present in the current learning exposure, the model will learn on all training chairs and tables.

at each learning exposure. We utilize SDFNet as the batch learner. All models are trained from random initialization.

Results. The results are shown in Figs. 2a and 2b for single and repeated exposures, respectively. For single exposure, both C-SDFNet and C-OccNet maintain their accuracy over time and even exhibit a slight upward trend of increasing accuracy. This is surprising since we are not taking any steps to ameliorate catastrophic forgetting and each learning exposure presents a significant domain shift, as the learner must incorporate information about the shape of a new class of objects. Since C-SDFNet and C-OccNet differ significantly in shape representation and are trained with different losses (L_1 loss for C-SDFNet and BCE loss for C-OccNet), we believe that *this finding likely reflects a basic property of the shape reconstruction problem* rather than the inductive biases of a particular model.

In the repeated exposures setting (Fig. 2b), the performance of both architectures when trained with 3-DOF VC *improves significantly over time*, and eventually performs on par with the batch learner (C-SDFNet and C-OccNet with GT D+N and C-SDFNet with Image).⁷ Unlike the experiments in [54], which showed similar asymptotic behavior for classification accuracy, these results were obtained *without* exemplar memory or other heuristics. Note that SDFNet trained with OC does not show a significant increase as 3-DOF VC representation over time. This complements the finding in [56] that training with 3-DOF VC results in a more robust feature representation.

3.2. Silhouette, Depth and Normal Maps Prediction

The task in Sec. 3.1 requires the learner to infer the global 3D structure of each object, with the best performance arising when depth+normals are given as input. Additional insights into continual reconstruction can be obtained from a task that requires 2D to 3D inference, but does not require the model to infer the self-occluded surfaces of the object. We therefore investigate the CL performance of 2.5D sketch estimation in the single exposure case, which entails learning to segment foreground/background and estimates the depth and surface normal maps, given a single RGB input image. We adopt the U-ResNet18-based MarrNet [58] architecture, referred to as C-MarrNet with an ILSVRC-2014 pre-trained ResNet18 for the image encoder.

We render ShapeNet13 with variations in lighting and surface reflectance against random backgrounds to obtain the input RGB images. We evaluate C-MarrNet using MSE as the error metric for D+N prediction and IoU for silhouette prediction. Fig. 3a demonstrates that single exposure silhouette prediction does not suffer catastrophic forgetting, and in fact the IoU increases over time. Likewise for D+N prediction in Fig. 3b, the MSE decreases over time for

depth estimation and remains the same for normal prediction. These findings corroborate the 3D shape reconstruction results from Fig. 2a, demonstrating the robustness of 2D to 3D reconstruction tasks to catastrophic forgetting.

3.3. Image Autoencoder

The tasks in Secs. 3.1 and 3.2 require the learner to solve a challenging 2D to 3D inference problem. In order to gain further insight, we conducted an additional experiment on continual image autoencoding, a reconstruction task that uses a simpler 2D to 2D mapping. We adapt SegNet [5] to continual training, resulting in C-SegNet. We experiment on CIFAR-100 (size 32×32) with one class per exposure and MSE per pixel as the error metric. Note that the model is trained from random initialization.

The result is shown in Fig. 4. The MSE per pixel decreases over time and eventually reaches that of the batch learner. The image in green at the top of the figure is a test image (not learned during training) from the CIFAR class that the learner sees in the first exposure. Reconstructions of this test image are shown at three different learning exposures, denoted by red arrows. Despite the fact that this class was seen only once in the first exposure (and starting from random weights), the model is nonetheless able to reconstruct it with high fidelity. This is yet more evidence for the robustness of continual reconstruction.

3.4. Discussion of Continual Reconstruction

We have identified (for the first time) a set of *continual reconstruction* tasks that do not suffer from forgetting, as evidenced by the results in Figs. 2, 3, and 4. These models were trained with *standard SGD*, without exemplar memory or other heuristics. One point of contact between classification and reconstruction is that both sets of tasks benefit significantly from *repeated exposures* (see Fig. 2b). While the object categories that define the exposures are not an explicit part of the reconstruction task, continual reconstruction is still a potentially challenging problem with significant domain shift. For example, the categories “chair” and “bowl” in ShapeNet define very different 3D data distributions with no parts in common. From this point of view, it is surprising that forgetting is not more widespread. In Sec. 5 we demonstrate the value of propagating the learned representation between exposures, but a complete explanation for our findings remains as a target for future work.

We now briefly discuss two potential limitations of our current findings. First, all of our reconstruction experiments, with the exception of image autoencoding, utilize synthetic 3D object models. This limits our ability to infer properties of reconstruction tasks *in general* from our current experiments. However, we point out that 3D shape reconstruction on synthetic images is still a very challenging computational problem, e.g. the SOTA result

⁷The 65 learning exposures (x axis) in Fig. 2b result from 13 ShapeNet classes divided by 2 classes per exposure with 10 repetitions each.

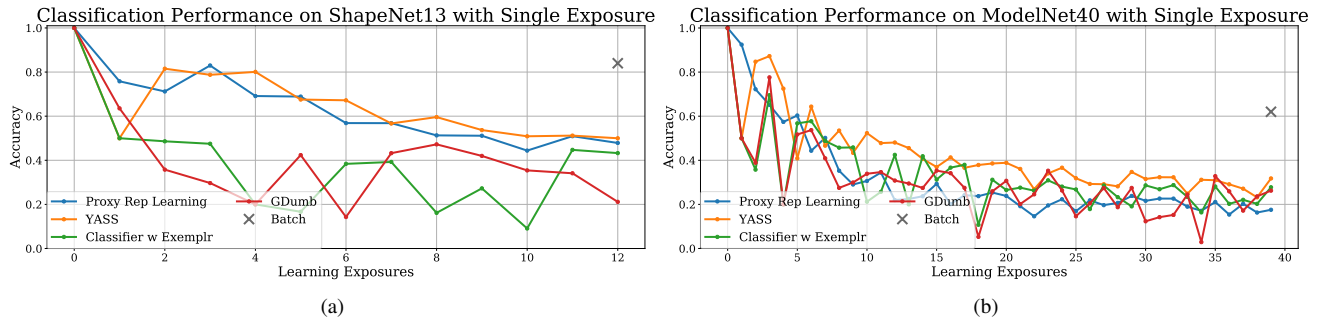


Figure 5: (a) Performance of proxy representation learning task (Proxy Rep Learning) in continual learning of classification on ShapeNet13 and (b) on ModelNet40. Proxy Rep Learning achieves competitive performance to SOTA baselines.

on ShapeNet13 is an FS@1 of 0.5 out of a maximum of 1.0 [56]. This in turn raises the second possible limitation, that the lack of forgetting may be tied in part to the fact that the models are not yet able to achieve very high accuracy. More accurate models might be more closely tuned to the data distribution in each exposure, increasing the potential for domain shift. While this might be true for 3D shape reconstruction, the depth+normals and autoencoder tasks are achieving a high level of accuracy, which provides a counterpoint to the argument. We hope this work will encourage the community to conduct additional investigations into this intriguing phenomenon.

4. Proxy Task for Continual Classification

The robustness of representation learning in reconstruction begs the question of whether it could be used as a proxy task to improve continual classification. We test that hypothesis here via a simple approach: We train a 3D reconstruction model continually as in Sec. 3.1, and at inference time we extract the feature from the image encoder of SDFNet VC GT D+N via a forward pass. We maintain an exemplar set of 20 images/class with class labels following the procedure from Sec. 5, which is not used at training time. Instead, we use the extracted representation to perform nearest-class-mean (NCM) classification with the exemplars at testing time. Specifically, the mean feature of each class is first computed from the exemplar set. Then test samples are assigned the label of the closest mean feature via cosine distance (Fig. 1). This provides a way to bootstrap a classifier from continual reconstruction.

We conduct experiments with ShapeNet13 and ModelNet40 with one class per exposure. We compare the performance of the proxy classifier against three baselines: YASS (Sec. 5), GDumb [42] and a standard classifier trained continually with cross entropy loss and the same exemplar set, denoted as Classifier with Exemplars. Fig. 5 illustrates that the proxy classifier using NCM outperforms the GDumb and Classifier with Exemplars on ShapeNet13, and achieves competitive performance with YASS on both datasets. This is a potentially interesting finding as it demonstrates that a significant amount of discriminative information is encoded

in the continual shape representation. This suggests that it may be profitable to explore other proxy tasks as a means to overcome catastrophic forgetting in classification.

5. YASS—Simple Baseline for Classification

Our findings in Secs. 3 and 4 have highlighted the robustness to forgetting in continual reconstruction, making it clear that effective approaches to incremental representation learning in classification remain a key challenge. In this section, we address the question of what exactly are the key ingredients in an effective approach to continual classification? Inspired by the work of [42], we present a simple baseline method for *class-incremental* classification, which we term YASS (Yet Another Simple baSeline). YASS encapsulates a minimal set of algorithmic components: using exemplars chosen at random, employing weighted gradient for balancing, classifying via the network output with cross-entropy loss, and importantly, applying continuous representation learning approach. YASS adapts standard batch learning to the continual learning context with the fewest changes. Surprisingly, we show that YASS achieves SOTA performance in the class-incremental single task setting.

Exemplar Memory and Management. As in [10, 46, 42, 59] we allow for a small (less than 3% of total training data) exemplar set. Similar to [42], rather than using complex heuristics like herding [46], we use random exemplar selection where the exemplar samples are randomly chosen from the learning data. In prior memory based algorithms the exemplar set size is fixed and equally split among all learned concepts which leads to unused memory⁸. To counter this issue, we equally divide the remaining exemplar slots to the first learned concepts.

With data balancing. To address the issue where the new training data significantly outnumbers stored exemplar data, we propose a data balancing mechanism based on a common method as described in [23] and refer to it as Weighted Gradient (WG). Specifically, we make sure that every class in the training data contributes equally during backpropaga-

⁸For example, when the exemplar set size is 2000 images, after the 91st concept is learned, each concept will evenly have 21 exemplars, which leaves 89 exemplar slots in the memory unused.

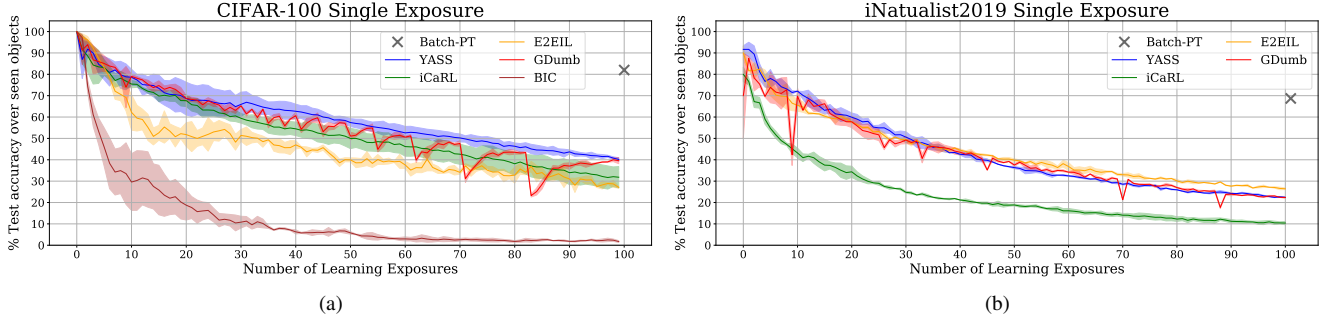


Figure 6: (a) Performance of YASS, iCaRL [46], E2EIL [10], GDumb [42], and BiC [59] when presented with a single exposure for each category from CIFAR-100 with 1 class learned per exposure. Performance is averaged over 3 runs with random class orderings. (b) YASS, iCaRL, E2EIL and GDumb on iNaturalist2019 in a single exposure setting with 10 classes learned per exposure. Performance is averaged over 2 runs. YASS outperforms others on CIFAR-100 and achieves competitive performance on iNaturalist-2019.

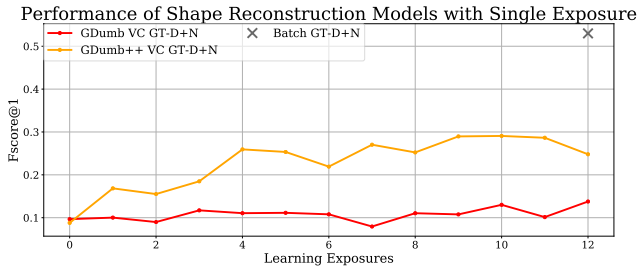


Figure 7: Performance of GDumb and GDumb++ in 3D shape reconstruction on ShapeNet13 with 1K exemplars (3.7% of training data). GDumb++ outperforms GDumb by a significant margin.

tion by scaling the gradients inversely proportionally to the number of samples of the corresponding class.

Experiments. We conduct experiments on two image datasets: CIFAR-100 [28] and the challenging large scale dataset, iNaturalist-2019 [21] with 1010 categories of highly similar species. We evaluate the performance of YASS against current state-of-the-art algorithms for class-incremental subtask that allow exemplar memory, classified as formulation B2 in [42]. Despite the simple design choices, YASS outperforms SOTA methods on the most challenging setting of CIFAR-100 (one class learned per exposure with 500 exemplars) in Fig. 6a and achieves competitive performance on iNaturalist-2019 dataset with 10 classes learned per exposure and 8080 exemplars in Fig. 6b. In the Appendix we demonstrate the performance of YASS on different exemplar set sizes and with repeated exposures.

Continuous Representation Discussion. YASS employs continuous representation learning, which is presumably one of the important keys to success. Conversely, GDumb is an episodic representation learner, designed to test the hypothesis that there is no value in representation propagation.⁹ Sec. 3 shows that reconstruction tasks demonstrate the benefit of continuous representation learning, as they do not suffer from catastrophic forgetting. While GDumb achieves competitive performance on classification task, it is not beneficial for shape learning (Fig. 7). We further im-

⁹The lack of benefit presumably arises because the biases introduced by domain shift and catastrophic forgetting outweigh the benefits.

plement a variant of GDumb called GDumb++, which differs from GDumb only in that it learns the representation continuously for 3D shape reconstruction task. Since both GDumb and GDumb++ are trained on the same amount of input data (given by the size K of the exemplar set), any performance gap is attributable to the value of propagating the learned representation. In Fig. 7, GDumb++ observes positive forward transfer, with the performance increases over time and significantly exceeds GDumb by 0.2 FS@1.

For classification, solely learning the representation continuously might not be sufficient.¹⁰ Different from prior continuous representation learning approaches like iCaRL, BiC or E2EIL, YASS allows the representation to be optimized over time instead of constraining the weights of the model on those learned from the previous exposures (eg. distillation loss), which might be a local minimum for all training data. By further carefully managing the exemplar set and making use of all the available training data with a data balancing strategy, YASS successfully illustrates the benefit of continuous feature representation learning for classification task and consistently achieves SOTA performance in different settings.

6. Feature Representation Learning Analysis

In this section, we analyze the dynamics of forgetting in the feature representation of CL classification. While prior works demonstrated that the FC layer is susceptible to forgetting due to domain shift during CL, we believe we are the first to thoroughly investigate and provide converging evidence on the forgetting of the evolving feature representation during class-incremental classification.

We utilize the feature representation of the model learned on all training data (batch model) as the “oracle”. We first extract the feature representation produced by the pooling layer prior to the final FC layer of both the CL models at each learning exposure and the batch model. Then, we com-

¹⁰We train the variant of GDumb as described above for the classification case and find its performance to be poor.

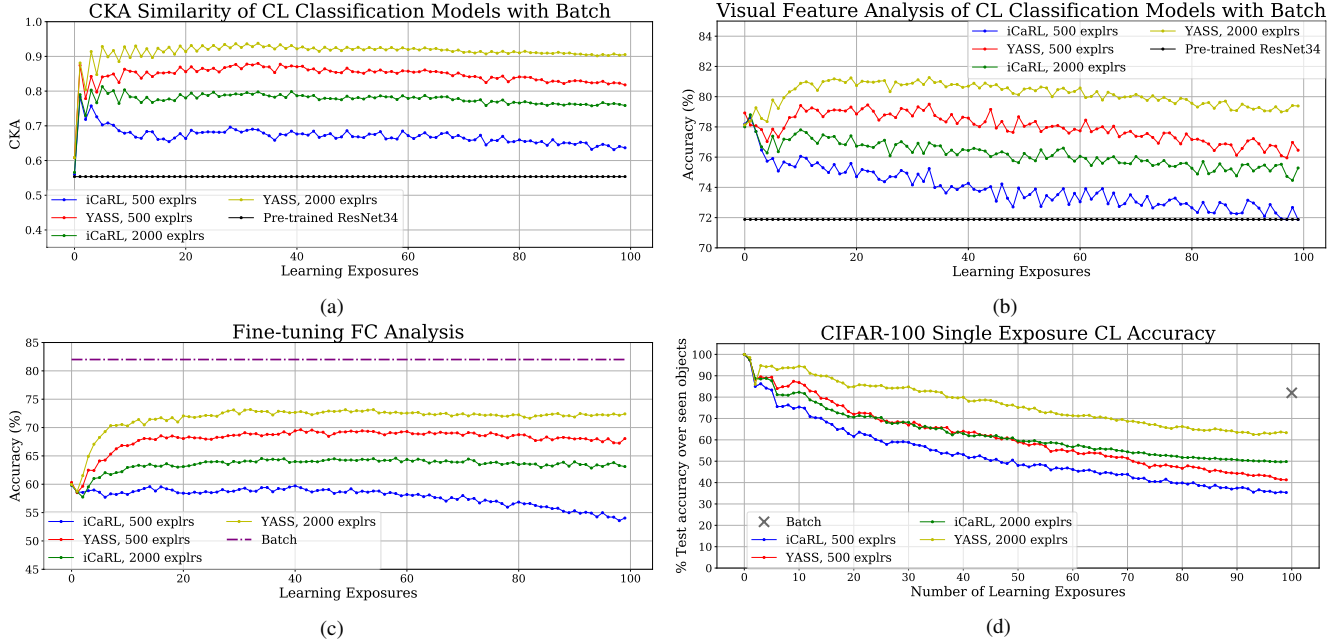


Figure 8: (a) CKA similarity analysis (b) VF analysis, (c) Fine-tuning FC analysis and (d) CL accuracy where the average performance of learned class is plotted at each learning exposure of different CL classification and batch models. Pre-trained ResNet34 indicates the representation extracted from ILSVRC-2014 pretrained ResNet34, which is the lower bound on the performance for CKA and VF. Feature representations of YASS and iCaRL perform significantly more stable over time in all cases compared to the CL accuracy.

pare these feature representations using CKA [27] and our novel visual feature analysis. CKA computes the correlation score (ranging from 0 to 1) between the feature representations. For visual feature analysis, we first define a set of binary attributes that we refer to as *visual features (VFs)*, that capture the information in the feature representation of the batch model. This is done by binary masking $\mathbb{1}\{a_i \geq t\}$ where a_i is each activation in the representation and t indicates the threshold.¹¹ We use the learned representation at each learning exposure to train a set of linear binary classifiers to predict each of the final target VFs (Fig. 1, last row). The intuition is that the accuracy of the VF classifiers measures the extent to which the current learned representation captures information related to the final representation. Please see Appendix for more details.

We further conduct an experiment in which the feature representation at each learning exposure is frozen and the FC layer is finetuned on all training data from both learned and future classes (Fine-tuning FC). Note that since the FC layer is trained with the same data at each learning exposure as the batch model, the performance of Fine-tuning FC indicates the robustness of the feature representation over time compared to the batch model.

Figs. 8a, 8b show that the feature representation learned by CL models do not suffer from catastrophic forgetting as much as the class outputs from the FC layer (as com-

¹¹Prior work on network quantization [15] has demonstrated that activations can be quantized without incurring a significant drop in accuracy.

pared to the significant downward trend of the curves in Fig. 8d). We confirm this finding by the result from Finetuning-FC (Fig. 8c) with the performance on all CL models very close to batch performance. Interestingly, while Figs. 8a, 8b, 8c demonstrate that the feature representation learned by YASS with 500 exemplars is more similar to the batch model than iCaRL with 2000 exemplars (red vs green curves), the CL average accuracy shows an opposite trend where YASS with 500 exemplars performs worse than iCaRL with 2000 exemplars over time.

7. Conclusion

We have established that there is a class of reconstruction tasks that does not exhibit catastrophic forgetting. Hence, the answer to the question we pose in our title “Does continual learning = catastrophic forgetting?” is “No”. However, it is clear that whether catastrophic forgetting happens depends on the task and the setting, e.g., classification tasks do exhibit forgetting in the single exposure case. We further illustrate the potential of utilizing the feature representations learned by shape reconstruction as a proxy task for CL of classification, which we have demonstrated to perform on par with the SOTA methods.

We show the benefit of learning representation continuously over episodically in CL of reconstruction. For classification, we identify the key ingredients for an effective continuous representation learning approach: careful exemplar management and data balance preservation during training.

We present a simple method, YASS based on standard SGD training with exemplars that gives SOTA performance.

We provide converging evidence using three different tools on the hypothesis that the feature representation is less prone to forgetting than the class outputs obtained from the FC layer. We release the codebase, all training data and trained models to the community at <https://github.com/rehg-lab/CLRec>.

8. Acknowledgement

We would like to thank Miao Liu, Zixuan Huang and Meera Hahn for the helpful discussion. This work was supported by NIH R01-MH114999 and NSF Award 1936970. This paper is dedicated to the memory of Chengming (Julian) Gu.

References

- [1] David Abel, Dilip Arumugam, Lucas Lehnert, and Michael Littman. State abstractions for lifelong reinforcement learning. In *International Conference on Machine Learning*, pages 10–19, 2018.
- [2] Guillaume Alain and Yoshua Bengio. Understanding intermediate layers using linear classifier probes. Technical report, 2016.
- [3] Rahaf Aljundi, Francesca Babiloni, Mohamed Elhoseiny, Marcus Rohrbach, and Tinne Tuytelaars. Memory aware synapses: Learning what (not) to forget. In *Proceedings of the European Conference on Computer Vision (ECCV)*, pages 139–154, 2018.
- [4] Rahaf Aljundi, Klaas Kelchtermans, and Tinne Tuytelaars. Task-free continual learning. In *Proceedings of the IEEE/CVF Conference on Computer Vision and Pattern Recognition (CVPR)*, June 2019.
- [5] Vijay Badrinarayanan, Alex Kendall, and Roberto Cipolla. Segnet: A deep convolutional encoder-decoder architecture for image segmentation. *IEEE transactions on pattern analysis and machine intelligence*, 39(12):2481–2495, 2017.
- [6] Yogesh Balaji, Mehrdad Farajtabar, Dong Yin, Alex Mott, and Ang Li. The Effectiveness of Memory Replay in Large Scale Continual Learning. Technical report, 2020.
- [7] Eden Belouadah and Adrian Popescu. Il2m: Class incremental learning with dual memory. In *Proceedings of the IEEE International Conference on Computer Vision*, pages 583–592, 2019.
- [8] Blender Online Community. *Blender - a 3D modelling and rendering package*. Blender Foundation, Blender Institute, Amsterdam.
- [9] Pietro Buzzega, Matteo Boschini, Angelo Porrello, Davide Abati, and Simone Calderara. Dark experience for general continual learning: a strong, simple baseline. In H. Larochelle, M. Ranzato, R. Hadsell, M. F. Balcan, and H. Lin, editors, *Advances in Neural Information Processing Systems*, volume 33, pages 15920–15930. Curran Associates, Inc., 2020.
- [10] Francisco M Castro, Manuel J Marin-Jimenez, Nicolas Guil, Cordelia Schmid, and Karteek Alahari. End-to-end incremental learning. In *Proceedings of the European Conference on Computer Vision (ECCV)*, pages 233–248, 2018.
- [11] Fabio Cermelli, Massimiliano Mancini, Samuel Rota Bulo, Elisa Ricci, and Barbara Caputo. Modeling the background for incremental learning in semantic segmentation. In *Proceedings of the IEEE/CVF Conference on Computer Vision and Pattern Recognition (CVPR)*, June 2020.
- [12] Angel X Chang, Thomas Funkhouser, Leonidas Guibas, Pat Hanrahan, Qixing Huang, Zimo Li, Silvio Savarese, Manolis Savva, Shuran Song, Hao Su, et al. Shapenet: An information-rich 3d model repository. *arXiv preprint arXiv:1512.03012*, 2015.
- [13] Arslan Chaudhry, Marc Aurelio Ranzato, Marcus Rohrbach, and Mohamed Elhoseiny. Efficient lifelong learning with a-GEM. In *International Conference on Learning Representations*, 2019.
- [14] Christopher B Choy, Danfei Xu, JunYoung Gwak, Kevin Chen, and Silvio Savarese. 3d-r2n2: A unified approach for single and multi-view 3d object reconstruction. In *European conference on computer vision*, pages 628–644. Springer, 2016.
- [15] Matthieu Courbariaux, Itay Hubara, Daniel Soudry, Ran El-Yaniv, and Yoshua Bengio. Binarized neural networks: Training deep neural networks with weights and activations constrained to+ 1 or-1. *arXiv preprint arXiv:1602.02830*, 2016.
- [16] Matthias De Lange, Rahaf Aljundi, Marc Masana, Sarah Parisot, Xu Jia, Ales Leonardis, Gregory Slabaugh, and Tinne Tuytelaars. A continual learning survey: Defying forgetting in classification tasks. *arXiv preprint arXiv:1909.08383*, 2019.
- [17] Arthur Douillard, Matthieu Cord, Charles Ollion, and Thomas Robert. Podnet: Pooled outputs distillation for small-tasks incremental learning. Springer, 2018.
- [18] Arthur Douillard, Matthieu Cord, Charles Ollion, Thomas Robert, and Eduardo Valle. Small-task incremental learning. *arXiv preprint arXiv:2004.13513*, 2020.
- [19] Mohamed Elhoseiny, Francesca Babiloni, Rahaf Aljundi, Marcus Rohrbach, Manohar Paluri, and Tinne Tuytelaars. Exploring the challenges towards lifelong fact learning. In *Asian Conference on Computer Vision*, pages 66–84. Springer, 2018.
- [20] Arthur Gretton, Olivier Bousquet, Alex Smola, and Bernhard Schölkopf. Measuring statistical dependence with hilbertschmidt norms. In *International conference on algorithmic learning theory*, pages 63–77. Springer, 2005.
- [21] Grant Van Horn, Oisin Mac Aodha, Yang Song, Yin Cui, Chen Sun, Alex Shepard, Hartwig Adam, Pietro Perona, and Serge Belongie. The inaturalist species classification and detection dataset, 2018.
- [22] Saihui Hou, Xinyu Pan, Chen Change Loy, Zilei Wang, and Dahua Lin. Learning a unified classifier incrementally via re-balancing. In *Proceedings of the IEEE Conference on Computer Vision and Pattern Recognition*, pages 831–839, 2019.

- [23] Nathalie Japkowicz and Shaju Stephen. The class imbalance problem: A systematic study. *Intelligent data analysis*, 6(5):429–449, 2002.
- [24] Xisen Jin, Junyi Du, and Xiang Ren. Gradient based memory editing for task-free continual learning. *arXiv preprint arXiv:2006.15294*, 2020.
- [25] Christos Kaplanis, Murray Shanahan, and Claudia Clopath. Continual reinforcement learning with complex synapses. *arXiv preprint arXiv:1802.07239*, 2018.
- [26] James Kirkpatrick, Razvan Pascanu, Neil Rabinowitz, Joel Veness, Guillaume Desjardins, Andrei A Rusu, Kieran Milan, John Quan, Tiago Ramalho, Agnieszka Grabska-Barwinska, et al. Overcoming catastrophic forgetting in neural networks. *Proceedings of the national academy of sciences*, 114(13):3521–3526, 2017.
- [27] Simon Kornblith, Mohammad Norouzi, Honglak Lee, and Geoffrey Hinton. Similarity of neural network representations revisited. *arXiv preprint arXiv:1905.00414*, 2019.
- [28] Alex Krizhevsky, Geoffrey Hinton, et al. Learning multiple layers of features from tiny images. 2009.
- [29] Karel Lenc and Andrea Vedaldi. Understanding Image Representations by Measuring Their Equivariance and Equivalence. *International Journal of Computer Vision*, 127(5):456–476, 2019.
- [30] Timothée Lesort, Hugo Caselles-Dupré, Michael Garcia-Ortiz, Andrei Stoian, and David Filliat. Generative models from the perspective of continual learning. In *2019 International Joint Conference on Neural Networks (IJCNN)*, pages 1–8. IEEE, 2019.
- [31] Yixuan Li, Jason Yosinski, Jeff Clune, Hod Lipson, and John Hopcroft. Convergent Learning: Do different neural networks learn the same representations? In *Proceedings of the International Conference on Learning Representations (ICLR 16)*, pages 1–21, 2016.
- [32] Xialei Liu, Chenshen Wu, Mikel Menta, Luis Herranz, Bogdan Raducanu, Andrew D Bagdanov, Shangling Jui, and Joost van de Weijer. Generative feature replay for class-incremental learning. In *Proceedings of the IEEE/CVF Conference on Computer Vision and Pattern Recognition Workshops*, pages 226–227, 2020.
- [33] Xialei Liu, Hao Yang, Avinash Ravichandran, Rahul Bhotika, and Stefano Soatto. Multi-task incremental learning for object detection, 2020.
- [34] Yaoyao Liu, Yuting Su, An-An Liu, Bernt Schiele, and Qianru Sun. Mnemonics training: Multi-class incremental learning without forgetting. In *Proceedings of the IEEE/CVF Conference on Computer Vision and Pattern Recognition*, pages 12245–12254, 2020.
- [35] David Lopez-Paz and Marc’Aurelio Ranzato. Gradient episodic memory for continual learning. In *Advances in neural information processing systems*, pages 6467–6476, 2017.
- [36] Davide Maltoni and Vincenzo Lomonaco. Continuous learning in single-incremental-task scenarios. *Neural Networks*, 116:56–73, 2019.
- [37] Lars Mescheder, Michael Oechsle, Michael Niemeyer, Sebastian Nowozin, and Andreas Geiger. Occupancy networks: Learning 3d reconstruction in function space. In *Proceedings of the IEEE Conference on Computer Vision and Pattern Recognition*, pages 4460–4470, 2019.
- [38] Umberto Michieli and Pietro Zanuttigh. Incremental learning techniques for semantic segmentation. In *Proceedings of the IEEE/CVF International Conference on Computer Vision (ICCV) Workshops*, Oct 2019.
- [39] Seyed Iman Mirzadeh, Mehrdad Farajtabar, Dilan Gorur, Razvan Pascanu, and Hassan Ghasemzadeh. Linear mode connectivity in multitask and continual learning. *arXiv preprint arXiv:2010.04495*, 2020.
- [40] Ari S. Morcos, Maithra Raghu, and Samy Bengio. Insights on representational similarity in neural networks with canonical correlation. In *Advances in Neural Information Processing Systems*, pages 5727–5736, 2018.
- [41] Cuong V Nguyen, Yingzhen Li, Thang D Bui, and Richard E Turner. Variational continual learning. *arXiv preprint arXiv:1710.10628*, 2017.
- [42] Ameya Prabhu, Philip HS Torr, and Puneet K Dokania. Gdumb: A simple approach that questions our progress in continual learning. In *ECCV*, 2020.
- [43] Maithra Raghu, Justin Gilmer, Jason Yosinski, and Jascha Sohl-Dickstein. SVCCA: Singular Vector Canonical Correlation Analysis for Deep Learning Dynamics and Interpretability. In *Proceedings Advances In Neural Information Processing Systems 31 (NIPS 2017)*, pages 1–17, 2017.
- [44] Vinay V Ramasesh, Ethan Dyer, and Maithra Raghu. Anatomy of catastrophic forgetting: Hidden representations and task semantics. *arXiv preprint arXiv:2007.07400*, 2020.
- [45] Dushyant Rao, Francesco Visin, Andrei Rusu, Razvan Pascanu, Yee Whye Teh, and Raia Hadsell. Continual unsupervised representation learning. In *Advances in Neural Information Processing Systems*, pages 7647–7657, 2019.
- [46] Sylvestre-Alvise Rebuffi, Alexander Kolesnikov, Georg Sperl, and Christoph H. Lampert. iCaRL: Incremental Classifier and Representation Learning. In *The IEEE Conference on Computer Vision and Pattern Recognition (CVPR)*, pages 5533–5542, July 2017.
- [47] Anthony Robins. Catastrophic Forgetting, Rehearsal and Pseudorehearsal. *Connection Science*, 7(2):123–146, 1995.
- [48] Andrei A Rusu, Neil C Rabinowitz, Guillaume Desjardins, Hubert Soyer, James Kirkpatrick, Koray Kavukcuoglu, Razvan Pascanu, and Raia Hadsell. Progressive neural networks. *arXiv preprint arXiv:1606.04671*, 2016.
- [49] Jonathan Schwarz, Jelena Luketina, Wojciech M Czarnecki, Agnieszka Grabska-Barwinska, Yee Whye Teh, Razvan Pascanu, and Raia Hadsell. Progress & compress: A scalable framework for continual learning. *arXiv preprint arXiv:1805.06370*, 2018.
- [50] Daeyun Shin, Charless C Fowlkes, and Derek Hoiem. Pixels, voxels, and views: A study of shape representations for single view 3d object shape prediction. In *Proceedings of the IEEE conference on computer vision and pattern recognition*, pages 3061–3069, 2018.
- [51] Hanul Shin, Jung Kwon Lee, Jaehong Kim, and Jiwon Kim. Continual learning with deep generative replay. In *Advances in Neural Information Processing Systems*, pages 2990–2999, 2017.

- [52] Konstantin Shmelkov, Cordelia Schmid, and Karteek Alahari. Incremental learning of object detectors without catastrophic forgetting. In *Proceedings of the IEEE International Conference on Computer Vision*, pages 3400–3409, 2017.
- [53] Karen Simonyan and Andrew Zisserman. Very deep convolutional networks for large-scale image recognition. *arXiv preprint arXiv:1409.1556*, 2014.
- [54] Stefan Stojanov, Samarth Mishra, Ngoc Anh Thai, Nikhil Dhanda, Ahmad Humayun, Chen Yu, Linda B Smith, and James M Rehg. Incremental object learning from contiguous views. In *Proceedings of the IEEE Conference on Computer Vision and Pattern Recognition*, pages 8777–8786, 2019. (Oral, Best Paper Finalist).
- [55] Maxim Tatarchenko, Stephan R Richter, René Ranftl, Zhuwen Li, Vladlen Koltun, and Thomas Brox. What do single-view 3d reconstruction networks learn? In *Proceedings of the IEEE Conference on Computer Vision and Pattern Recognition*, pages 3405–3414, 2019.
- [56] Anh Thai, Stefan Stojanov, Vijay Upadhyaya, and James M Rehg. 3d reconstruction of novel object shapes from single images. *arXiv preprint arXiv:2006.07752*, 2020.
- [57] Chenshen Wu, Luis Herranz, Xialei Liu, Joost van de Weijer, Bogdan Raducanu, et al. Memory replay gans: Learning to generate new categories without forgetting. In *Advances in Neural Information Processing Systems*, pages 5962–5972, 2018.
- [58] Jiajun Wu, Yifan Wang, Tianfan Xue, Xingyuan Sun, Bill Freeman, and Josh Tenenbaum. Marrnet: 3d shape reconstruction via 2.5 d sketches. In *Advances in neural information processing systems*, pages 540–550, 2017.
- [59] Yue Wu, Yinpeng Chen, Lijuan Wang, Yuancheng Ye, Zicheng Liu, Yandong Guo, and Yun Fu. Large scale incremental learning. In *Proceedings of the IEEE Conference on Computer Vision and Pattern Recognition*, pages 374–382, 2019.
- [60] Zhirong Wu, Shuran Song, Aditya Khosla, Fisher Yu, Linguang Zhang, Xiaoou Tang, and Jianxiong Xiao. 3d shapenets: A deep representation for volumetric shapes. In *Proceedings of the IEEE conference on computer vision and pattern recognition*, pages 1912–1920, 2015.
- [61] Jianxiong Xiao, James Hays, Krista A Ehinger, Aude Oliva, and Antonio Torralba. Sun database: Large-scale scene recognition from abbey to zoo. In *2010 IEEE Computer Society Conference on Computer Vision and Pattern Recognition*, pages 3485–3492. IEEE, 2010.
- [62] Ju Xu and Zhanxing Zhu. Reinforced continual learning. In *Advances in Neural Information Processing Systems*, pages 899–908, 2018.
- [63] Qiangeng Xu, Weiyue Wang, Duygu Ceylan, Radomir Mech, and Ulrich Neumann. Disn: Deep implicit surface network for high-quality single-view 3d reconstruction. 2019.
- [64] Jaehong Yoon, Saehoon Kim, Eunho Yang, and Sung Ju Hwang. Scalable and order-robust continual learning with additive parameter decomposition. In *International Conference on Learning Representations*, 2019.
- [65] Jaehong Yoon, Eunho Yang, Jeongtae Lee, and Sung Ju Hwang. Lifelong learning with dynamically expandable networks. *arXiv preprint arXiv:1708.01547*, 2017.
- [66] Lu Yu, Bartłomiej Twardowski, Xialei Liu, Luis Herranz, Kai Wang, Yongmei Cheng, Shangling Jui, and Joost van de Weijer. Semantic drift compensation for class-incremental learning. In *Proceedings of the IEEE/CVF Conference on Computer Vision and Pattern Recognition (CVPR)*, June 2020.
- [67] Friedemann Zenke, Ben Poole, and Surya Ganguli. Continual learning through synaptic intelligence. *Proceedings of machine learning research*, 70:3987, 2017.
- [68] Junting Zhang, Jie Zhang, Shalini Ghosh, Dawei Li, Serafettin Tasci, Larry Heck, Heming Zhang, and C-C Jay Kuo. Class-incremental learning via deep model consolidation. In *The IEEE Winter Conference on Applications of Computer Vision*, pages 1131–1140, 2020.
- [69] Xiuming Zhang, Zhoutong Zhang, Chengkai Zhang, Joshua B Tenenbaum, William T Freeman, and Jiajun Wu. Learning to Reconstruct Shapes from Unseen Classes. In *Advances in Neural Information Processing Systems (NeurIPS)*, 2018.
- [70] Bowen Zhao, Xi Xiao, Guojun Gan, Bin Zhang, and Shu-Tao Xia. Maintaining discrimination and fairness in class incremental learning. In *Proceedings of the IEEE/CVF Conference on Computer Vision and Pattern Recognition*, pages 13208–13217, 2020.

A. Datasets

A.1. ShapeNetCore.v2 & ModelNet40

Datasets: ShapeNetCore.v2 consists of 55 categories with 52K CAD models. This is the current largest 3D shape dataset with category labels. Many prior works in 3D shape reconstruction [37, 14] utilized a subset of 13 largest categories—ShapeNet13, which consists of approximately 40K 3D instances. Tbl. 2 lists the 13 categories and the number of samples in each category. For ShapeNet13, we use the standard train/val/test split from prior shape reconstruction works [14, 37]. We sample 100 objects/category from the test split for evaluation in the repeated exposures case. For the remaining 42 classes in ShapeNetCore.v2, we split randomly with proportion 0.7/0.1/0.2 for train/val/test splits. In the single exposure case on all classes of ShapeNetCore.v2, we randomly sample 30 objects/category for testing.

ModelNet40 consists of 40 categories with 12K object instances in total.

Rendering: We render 25 views of RGB images, ground truth silhouette, depth and surface normal maps with resolution 256×256 for each object. Following [56], we generate data using Cycles ray-tracing engine in Blender [8] with 3 degree-of-freedom, varying camera azimuth $\theta \in [0, 360^\circ]$, elevation $\phi \in [-50^\circ, 50^\circ]$ and tilt. For experiments with RGB images as inputs, we render with varying light, specular surface reflectance and random backgrounds from SUN Scenes [61].

SDF Point Sampling Strategy: For 3D shape reconstruction, training 3D points are sampled more densely close to the surface of the mesh. Following [56], we sample half of the training points within a distance of 0.03 to the surface, 30% with distance in the range $[0.03, 0.1]$ and 20% in the range $[0.1, 1.1]$. To train and evaluate OccNet, we obtain mesh occupancy values by binary masking $\mathbb{1}\{sdf \leq i\}$ where i is the isosurface value.

A.2. CIFAR-100

This is a standard image dataset consisting of 100 categories with 500 training and 100 testing samples for each category. Each image is of resolution 32×32 . In our experiment for classification baselines with repeated exposures, 60 categories are chosen randomly from 100 categories, which we denote as CIFAR-60.

A.3. iNaturalist-2019

This is a challenging large scale image dataset introduced in the FGVC6 workshop at CVPR 2019 as a species classification challenge. This dataset consists of 1010 categories of highly similar species which contains in total 268,243 images. iNaturalist is highly imbalanced and comprises of 6 super categories, each is further divided into

ID	Name	Num samples
02691156	airplane	4045
02828884	bench	1813
02933112	cabinet	1571
02958343	car	3532
03001627	chair	6778
03211117	display	1093
03636649	lamp	2318
03691459	loudspeaker	1597
04090263	rifle	2373
04256520	sofa	3173
04379243	table	8436
04401088	telephone	1089
04530566	watercraft	1939
	Total	39,757

Table 2: Statistics of ShapeNet13.

smaller categories (Table 3). In our experiments, we train on all 1,010 classes, with the average of 263 training images and standard deviation of 167.5.

Super-class	Num. Classes	Num. Images
Amphibians	10	3,912
Birds	126	47,867
Fungi	12	2,284
Insects	141	41,204
Plants	682	158,463
Reptiles	39	14,513
Total	1,010	268,243

Table 3: Statistics of iNaturalist-2019.

B. Description of Algorithms

B.1. Single-view 3D Shape Reconstruction

Architecture: We adapt SDFNet [56] and OccNet [37] for continual training, termed C-SDFNet and C-OccNet respectively. The architecture consists of an image encoder which is a ResNet-18 initialized with random weights and a point module which are multiple blocks of fully-connected layers with ReLU activation. Conditional Batch Normalization is used as applying an affine transformation on the output of the point module, conditioned on the 256-dimensional feature vector produced by the image encoder.

Loss function: C-SDFNet uses L_1 loss as the loss function, with high weights for points close to the surface. Specifically,

$$\mathcal{L}(s, \hat{s}) = \begin{cases} |s - \hat{s}|, & \text{if } |s| > 0.01 \\ 4|s - \hat{s}|, & \text{otherwise} \end{cases}$$

where s is the ground truth SDF value and \hat{s} is the predicted SDF value.

C-OccNet uses Binary Cross Entropy (BCE) loss on each input 3D point. Specifically,

$$\mathcal{L}(p, \hat{p}) = -p \log \hat{p} - (1 - p) \log(1 - \hat{p})$$

where $p \in \{0, 1\}$ is the ground truth binary value and \hat{p} is the predicted probability of whether a point is inside or outside the mesh.

Mesh generation: We use MISE, an algorithm that hierarchically extracts the mesh isosurface introduced by [37] to generate the predicted mesh. Instead of generating the SDF/occupancy values for all the points uniformly sampled in the cube, MISE starts from a lower resolution and hierarchically determines the voxels that contain the mesh to subdivide until the desired resolution is reached. We adapt MISE to work on both SDF and occupancy values.

Metric: Following [55, 56], we use F-Score at 1% as our main evaluation metric. We first sample 300K and 100K points respectively on the surface of the predicted mesh (S_1) and ground truth mesh (S_2). The metric is computed as the following

$$FS@1 = \frac{2 \cdot prec@1 \cdot rec@1}{prec@1 + rec@1}$$

where $prec@1$ is the precision at 1%, which measures the portion of points from S_1 that lie within a threshold 0.01 to the points from S_2 (in the case where the mesh is normalized to fit in a unit cube) and $rec@1$ is the recall at 1%, which measures the portion of points from S_2 that lie within a threshold 0.01 to the points from S_1 .

B.2. Silhouette, Depth and Normals Prediction

Architecture: We adapt the 2.5D sketch estimation from MarrNet [58] for continual training which we referred to as C-MarrNet. The backbone architecture for C-MarrNet is a U-ResNet18 with the ResNet18 image encoder initialized with ILSVRC-2014 pre-trained weights.

Loss functions: We use MSE as the loss function for depth and normals prediction and BCE as the loss function for silhouette prediction.

Metrics: We use MSE as the main error for depth and normals prediction and Intersection-over-Union (IoU) for silhouette prediction. Specifically,

$$MSE(I, \hat{I}) = \frac{1}{K \times K} \sum_{i,j} \|I(i, j) - \hat{I}(i, j)\|_2^2$$

$$IoU(I, \hat{I}) = \frac{|I \cap \hat{I}|}{|I \cup \hat{I}|}$$

where I and \hat{I} are the ground truth and predicted images respectively.

B.3. Image Autoencoder

Architecture: We adapt SegNet [5] for continual image autoencoding, termed as C-SegNet. This model has an encoder network that consists of 13 convolutional layers that correspond to 13 layers of the VGG16 [53] network, initialized from scratch. Each layer of the decoder has a corresponding layer in the encoder network. The final layer of the decoder predicts values for 3 channels (red, green, blue) of each pixel.

Loss function: We train C-SegNet with MSE loss for each pixel, defined as

$$\mathcal{L}(I, \hat{I}) = \frac{1}{K \times K \times 3} \sum_{c=1}^3 \sum_{i,j} \|I(i, j, c) - \hat{I}(i, j, c)\|_2^2$$

where K is the size of the input image and $c = \{1, 2, 3\}$ is the 3 input channels (red, green, blue).

Metric: We use MSE as the main evaluation metric for the image autoencoding experiment.

B.4. Classification Baselines

iCaRL [46] addresses catastrophic forgetting by utilizing distillation loss in addition to classification loss on learned classes. Every time a new set of classes is introduced, the fully-connected layer is expanded with an output sigmoid unit for each new class. We then try to minimize the following loss

$$\mathcal{L}(w) = \mathcal{L}_D(w) + \mathcal{L}_C(w)$$

with $\mathcal{L}_D(w)$ is the distillation loss, defined by

$$\mathcal{L}_D(w) = \frac{-1}{N} \sum_{i=1}^N \sum_{j=1}^{C-1} (p_{i,j}^d \log q_{i,j} + (1 - p_{i,j}^d) \log(1 - q_{i,j}))$$

and $\mathcal{L}_C(w)$ is the classification loss defined by

$$\mathcal{L}_C(w) = \frac{-1}{N} \sum_{i=1}^N (p_{i,C} \log q_{i,C} + (1 - p_{i,C}) \log(1 - q_{i,C}))$$

where N is the number of total training samples in the mini-batch, C is the total number of classes seen, p_i^d is the output of the model from the previous exposure (before any update on w) of sample i , $p_{i,C}$ is the ground truth label for sample i and q_i is the current model's predicted output of sample i .

iCaRL further allows for a small explicit memory to store samples from the learned classes. At each learning exposure, explicit memory will be combined with the current training data to form a new training set. Exemplar memory is chosen by a herding algorithm, where the chosen samples for each class are the closest to the mean feature of the class in the feature space. Despite being trained with a classifier layer, during inference time, iCaRL classifies test samples

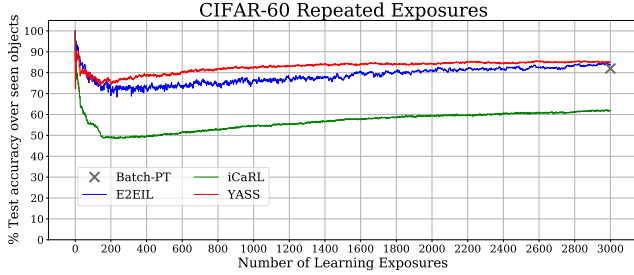


Figure 9: Performance of YASS, iCaRL, E2EIL and GDumb on CIFAR-60 with repeated exposures. YASS demonstrates a strong performance over SOTA methods.

using nearest class mean (NCM) classifier operating in the feature space.

E2EIL [10] builds on top of iCaRL. The major difference is that E2EIL is trained end-to-end with network outputs used for classification. To address the issue of class imbalance where the current training data outnumbers exemplar memory, E2EIL proposes balanced finetuning. Specifically, the model is first trained on the combined training data, then an exemplar set is chosen using herding algorithm, similar to iCaRL. After that, in the balanced finetuning phase, the model is trained on the exemplar set with the same number of samples for each class. The final exemplar set is then chosen again at the end of balanced finetuning phase. E2EIL utilizes an extensive data augmentation strategy during training which creates 12 copies of each image with a combination of transformations like random cropping, horizontal flipping, etc.

In our experiments, we used the PyTorch implementation of iCaRL and E2EIL released with [54].¹²

BiC [59] builds on the previous continual learning baselines, where exemplar memory and distillation loss are used to prevent catastrophic forgetting. The paper identifies that the FC layer is significantly more biased towards the current training data. As a resolution, the authors propose a bias correction layer, where two bias parameters α and β are learned for the new classes at each learning exposure. Specifically, the model is first trained with exemplar memory, standard cross entropy loss and distillation loss. In the second stage, the convolutional layers and the FC layer are frozen, and the two bias parameters are estimated using a small validation dataset. BiC uses the standard softmax with cross entropy loss to optimize the bias parameters. We adapted the PyTorch implementation of BiC¹³ to work on our setting.

GDumb [42] is a simple algorithm that randomly selects exemplars and performs training on the exemplar set only. At each learning exposure, the model is trained from scratch

on the exemplar set, in which each category is represented with the same number of samples. GDumb utilizes the standard cross-entropy loss and classifies using the network outputs. We used our PyTorch implementation of GDumb so that we can compare the different algorithms using the same backbone architecture.

Following [54], we train the model with ILSVRC-2014 pre-trained ResNet34. The input images are resized to resolution 224×224 . For the single exposure case, all the training samples from a subset of categories are present to the learners at each learning exposure. Specifically, for CIFAR-100, the CL models learn on 1 category at a time and for iNaturalist-2019, 10 categories are present to the CL models at each learning exposure. For repeated exposures on CIFAR-60, we sample with replacement 100 training images at each learning exposure. Each class is repeated 50 times, resulting in a total of 3000 learning exposures on 60 classes of the CIFAR-100 dataset.

C. Hyperparameter Settings

Tbl. 4 shows the hyperparameters used to train the algorithms present in the paper.

D. Additional Results for YASS

In this section, we first provide additional evidence that YASS outperforms other baselines on CIFAR-60 dataset with repeated exposures. In this experiment, each of the 60 classes is present 50 times. The exemplar set size is 1600, which is approximately 5.3% of the training set. We compare YASS against iCaRL [46] and E2EIL [10] as in [54]. YASS outperforms these methods in the repeated exposures case (Fig. 9). Since YASS, E2EIL and iCaRL are continuous representation learning approaches, the feature representation is refined when a category is exposed again and thus, demonstrating an increasing trend in the performance and eventually reaching that of the batch model (for YASS and E2EIL). Additionally, we compare YASS against GDumb, an episodic representation learning approach. Since GDumb is trained from scratch at each learning exposure, the feature representation does not benefit from repetition. YASS and E2EIL outperforms GDumb by 15% at the end, demonstrating the advantage of the continuous over the episodic representation learning approach in the repeated exposures case.

We further demonstrate the consistently strong performance of YASS with different number of exemplar set sizes (Fig. 10). We evaluate the performance of different SOTA methods on CIFAR-100 in the single exposure case, with 1000 exemplars (Fig. 10a) and 2000 exemplars (Fig. 10b). YASS outperforms iCaRL, E2EIL and BiC in both cases. GDumb shows a significant benefit from having more exemplars, as its performance approaches that of YASS when

¹²<https://github.com/iolfcv/experiments>

¹³<https://github.com/sairin1202/BiC>

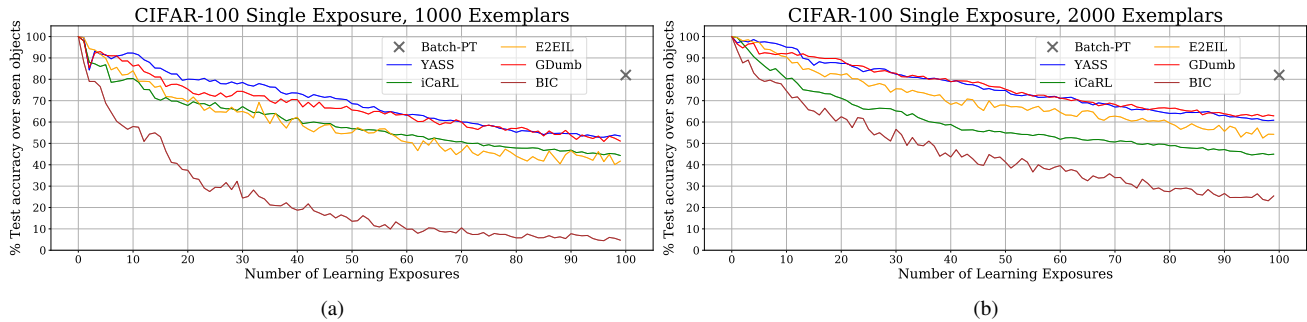


Figure 10: (a) Performance of YASS, iCaRL, E2EIL and GDumb on CIFAR-100 in the single exposure case with 1000 exemplars. (b) with 2000 exemplars. YASS demonstrates a consistently strong performance over SOTA methods.

Algorithm	Optimizer	LR	Scheduler	WD	Num epochs	Minibatch size
3D Shape Rec	Adam	0.0001	N/A	0	500	128
Silhou, D+N Pred	Adam	0.0001	N/A	0	500	50
Image Autoenc	Adam	0.0001	N/A	0	250	200
YASS-CIFAR	SGD	0.002	N/A	$1e^{-5}$	5	200
GDumb-CIFAR	SGD	0.05	CosineAnnealingLR, $T_{max} = 256$, $eta_{min} = 0.0005$, with warm start [42]	$1e^{-6}$	70	200
GDumb-Shape	Adam	0.0001	N/A	0	500	128
iCaRL-CIFAR	SGD	0.002	N/A	$1e^{-5}$	5	200
E2EIL-CIFAR	SGD	0.002	N/A	$1e^{-5}$	5, finetune 5	200
BiC-CIFAR	SGD	0.1	StepLR, step size = 70, gamma = 0.1	$2e^{-4}$	70	128
YASS-iNaturalist2019	SGD	0.002	Reduce by factor of 10 at learning expo- sure 10 & 20	$1e^{-5}$	20	200
iCaRL-iNaturalist2019	SGD	0.002	Reduce by factor of 10 at learning expo- sure 10 & 20	$1e^{-5}$	20	200
E2EIL-iNaturalist2019	SGD	0.002	Reduce by factor of 10 at learning expo- sure 10 & 20	$1e^{-5}$	15, finetune 5	200
BiC-iNaturalist2019	SGD	0.1	StepLR, step size = 70, gamma = 0.1	$2e^{-4}$	70	128

Table 4: Hyperparameter settings for the experiments present in the paper.

we increase the number of exemplars allowed.

E. Additional Explanation for Feature Representation Learning Analysis

In this section, we provide a more detailed explanation for the feature representation learning analyses done in the main text. To generate the curves in the analyses, we compare the feature representations obtained from the model trained on all training data (batch model) and the ones from the CL models at each learning exposure. Given the trained

batch model, we extract the feature representation $A^{(B)}$ produced by the last pooling layer before the FC layer that outputs the class predictions. The representation learned by the CL models at each learning exposure t , $A^{(t)}$ is obtained in a similar way.

E.1. CKA Similarity Analysis

Centered Kernel Alignment (CKA) introduced in [27] is a feature representation similarity measurement. Specifically, given feature representations X and Y with N neu-

rons, CKA is computed as

$$\text{CKA}(X, Y) = \frac{\text{HSIC}(X, Y)}{\sqrt{\text{HSIC}(X, X) \text{HSIC}(Y, Y)}}$$

where HSIC is the Hilbert-Schmidt Independence Criterion [20]. CKA similarity outputs range from 0 to 1, where 0 and 1 indicate the least and the most correlation between the feature representations respectively. In our experiments, we use the RBF CKA.

E.2. Visual Feature Analysis

The architecture for training the visual feature analysis approach is illustrated in Fig. 11. Given an input image, we first obtain the visual feature (VF) targets $Y^{(B)}$. This is done by binarizing the output of the average pooling layer $A^{(B)}$ using $\mathbb{1}\{a_i^{(B)} > \theta\}$ of the batch model, where a_i is each activation and θ is the threshold. For the experiments shown in the main text, we utilized threshold $\theta = 1$. The VF target with value 1 indicates that the visual feature is active and 0 otherwise. Our goal is to train a set of N binary classifiers where N is the number of visual features. After obtaining the feature representation learned at each learning exposure, we then freeze the weights of the feature extractor and train the VF classifier by optimizing the parameters ϕ_t of the FC layer $F^{(t)}$ to produce the VF prediction $\hat{Y}^{(t)}$ (blue branch in Fig. 11). Note that $F^{(t)}$ is different from the FC layer that outputs the class prediction (gray branch in Fig. 11). We use binary cross entropy loss on each element of the predicted VF outputs $\hat{Y}^{(t)}$ and the ground truth VF targets $Y^{(B)}$.

E.3. Finetuning FC Analysis

Given a trained model at each learning exposure t , we freeze the weights of the feature extractor up to the last pooling layer before the FC layer that produces the class outputs and train a new FC layer on all training data. This includes the data from the classes learned up to exposure t as well as the future classes. Note that this experiment is different from the experiments done in [59] since they only train on the data of the classes learned *up to* exposure t .

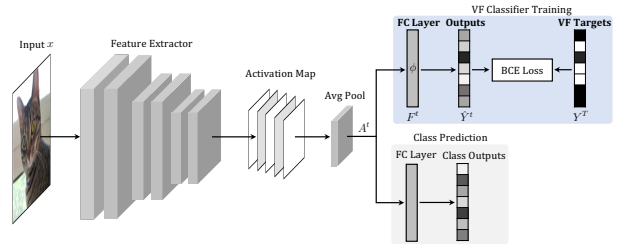


Figure 11: Architecture for the visual feature analysis. We freeze the weights of the feature extractor up to the pooling layer before the FC layer that outputs the class predictions. We train the VF classifier by optimizing the parameters ϕ_t of the FC layer $F^{(t)}$ (blue branch, top). The VF targets are obtained by binarizing the feature representation of the batch model. We utilize the binary cross entropy loss on each element of the predicted VF outputs $\hat{Y}^{(t)}$ and the ground truth VF targets $Y^{(B)}$. Please refer to the text for more details.